

# Major excursions in sulfur isotopes linked to permafrost change in Eurasia during the last 50,000 years

Received: 6 February 2023

Accepted: 1 July 2025

Published online: 1 August 2025



Rhiannon E. Stevens<sup>1</sup>✉, Hazel Reade<sup>1</sup>, Kerry L. Sayle<sup>2</sup>, Jennifer A. Tripp<sup>3</sup>, Delphine Frémondeau<sup>1</sup>, Adrian Lister<sup>4</sup>, Ian Barnes<sup>4</sup>, Mietje Germonpré<sup>5</sup>, Martin Street<sup>6</sup>, Julian B. Murton<sup>7</sup>, Simon H. Bottrell<sup>8</sup>, Daniel H. James<sup>1</sup> & Thomas F. G. Higham<sup>9,10</sup>

We identify a major sulfur isotope excursion in Eurasian faunal bone collagen from the last 50,000 years, here termed the Late Pleniglacial Sulfur Excursion. Our analysis suggests this is linked to changing permafrost conditions, presenting the utility of faunal collagen  $\delta^{34}\text{S}$  as a proxy for permafrost dynamics, a critical component of the global carbon cycle. Our findings complicate the use of archaeological faunal sulfur isotopes for mobility and palaeodietary studies.

Over the past two decades, sulfur isotope ratios ( $\delta^{34}\text{S}$ ) in plant, animal and human tissues have been increasingly used to explore food provenance, present and past diets and human and animal mobility. Most studies use sulfur isotopes as a geolocator, leveraging the spatial variability observed in plant sulfur isotope values, reflecting those of bioavailable sulfur. This variability arises because soil sulfur is primarily derived from mineral weathering of parent bedrock, the  $\delta^{34}\text{S}$  of which varies by rock type<sup>1</sup>. Additionally, the atmosphere contributes sulfur to soils (via dry deposition,  $\text{SO}_4^{2-}$  aerosols or wet deposition of  $\text{SO}_4^{2-}$ ), although pre-industrial atmospheric inputs contributed <10% of total soil S, excepting narrow zones of strong coastal seawater sulfate spray influence<sup>1,2</sup>. Recent studies suggest that waterlogged soil conditions may result in distinct bioavailable  $\delta^{34}\text{S}$  values<sup>3,4</sup>. Minimal fractionation is seen in organic-bound sulfur as it is passed along the food chain ( $\Delta^{34}\text{S}_{\text{tissue-diet}} \approx 0\text{‰}$  (refs. 5,6)), so animal  $\delta^{34}\text{S}$  values closely reflect those of the bioavailable  $\delta^{34}\text{S}$  at the base of their food chain<sup>7,8</sup>. Thus, animal  $\delta^{34}\text{S}$  values have been used to determine origin or mobility/migratory behaviours. Others use sulfur isotopes as a (palaeo)dietary indicator, as marine resources have high and relatively homogeneous  $\delta^{34}\text{S}$  values (about 20‰), whereas terrestrial  $\delta^{34}\text{S}$  tends to be lower and

more variable<sup>8</sup>. Overall, animal and human  $\delta^{34}\text{S}$  values are commonly interpreted as reflecting one or more stable sources, uninfluenced by environmental change, whereas a few studies argue that archaeological  $\delta^{34}\text{S}$  values reflect locally variable hydrological dynamics<sup>9–11</sup>.

Here we report results of 796  $\delta^{34}\text{S}$  isotope and 691 accelerator mass spectrometry (AMS) radiocarbon analyses from Late Pleistocene and Holocene fauna from Eurasia (Figs. 1 and 2, Supplementary Discussion 1.1 and Supplementary Data 1). One hundred and five samples come from contexts previously AMS dated. Our results show a high-magnitude excursion in faunal  $\delta^{34}\text{S}$  isotope values between approximately 30 and 15 thousand years (kyr) before present (BP) in some regions of Eurasia (Fig. 2 and Supplementary Fig. 1). This period corresponds to the latter part of the last ice age across much of Marine Isotope Stage 2 (about 29–11.7 kyr BP), including the Last Glacial Maximum (LGM, about 26.5–19 kyr BP). This excursion, which we name the Late Pleniglacial Sulfur Excursion (LPSE), is particularly pronounced in regions where we have good temporal coverage within a discrete geographic area, such as in Britain and Belgium, and is also evident in other regions, such as central Europe north of the Alps (Fig. 3 and Supplementary Fig. 2). However, the temporal and spatial coverage

<sup>1</sup>UCL Institute of Archaeology, London, UK. <sup>2</sup>Scottish Universities Environmental Research Centre, Rankine Avenue, East Kilbride, UK. <sup>3</sup>Department of Chemistry, University of San Francisco, San Francisco, CA, USA. <sup>4</sup>Department of Earth Sciences, Natural History Museum, London, UK. <sup>5</sup>Royal Belgian Institute of Natural Sciences, Brussels, Belgium. <sup>6</sup>MONREPOS Archaeological Research Center and Museum for Human Behavioural Evolution, Römisch-Germanisches Zentralmuseum, Leibniz-Research Institute for Archaeology, Neuwied, Germany. <sup>7</sup>Department of Geography, University of Sussex, Brighton, UK. <sup>8</sup>School of Earth and Environment, University of Leeds, Leeds, UK. <sup>9</sup>Department of Evolutionary Anthropology, Faculty of Life Sciences, University of Vienna, Vienna, Austria. <sup>10</sup>Human Evolution and Archaeological Sciences Forschungsverbund, University of Vienna, Vienna, Austria. ✉e-mail: [Rhiannon.Stevens@ucl.ac.uk](mailto:Rhiannon.Stevens@ucl.ac.uk)

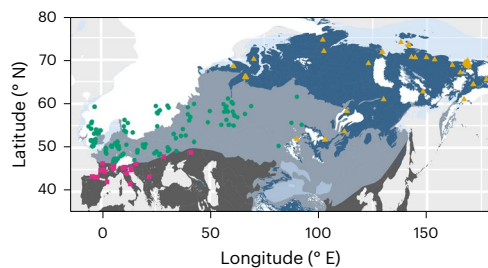


**Fig. 1 | Geographical distribution of the faunal samples.** Pale blue area indicates approximate zone of continuous permafrost at the LGM<sup>20</sup>. White area indicates LGM extent of ice sheets and glaciers<sup>40</sup>. Dark blue area indicates zone of present-day continuous and discontinuous permafrost distribution<sup>41</sup>. Pink squares: samples collected from regions where no permafrost was present during the last 50,000 years. Green circles: samples collected from areas that either had permafrost present or were under ice sheets/alpine glaciers at the LGM but where permafrost/ice sheets/alpine glaciers are absent today. Yellow triangles: samples collected from regions in which permafrost has been present throughout the past 50,000 years.

prevent us from determining whether the LPSE is time transgressive across this region. The LPSE occurs across multiple species with differing dietary niches and mobility behaviours (Fig. 2). The LPSE magnitude is substantial (up to 35‰), more than double that typically considered to indicate location-based differences<sup>12</sup>. This suggests that underlying continental-scale processes substantially impacted the terrestrial sulfur cycle during the Late Pleistocene.

Our Eurasian samples span the last 50 kyr (Fig. 1). The climate between about 50 and 28 kyr BP (Middle Pleniglacial) featured millennial-scale oscillations between cold stadial and mild interstadial states and fluctuating sea levels, superimposed on a long-term trend towards colder conditions and lower sea levels<sup>13,14</sup>. The Middle Pleniglacial environment across northwest and central Europe was wet and densely vegetated, with long periods of seasonal frost, and some discontinuous permafrost<sup>15,16</sup>. The onset of the Late Pleniglacial (about 28–14.7 kyr BP) saw the major expansion of European ice sheets<sup>17,18</sup>. Maximum ice-sheet extent occurred during the LGM, when sea levels were about 130 m lower than today<sup>19</sup>. Continuous permafrost (ground that remains  $\leq 0^\circ\text{C}$  for at least two consecutive years) was widespread across northern Eurasia at this time<sup>20</sup>. Between about 25 and 22 kyr BP, increasing aridity in northern Europe induced widespread fluvio-aeolian deposition in river valleys<sup>21</sup>, with maximum aridity between about 17 and 15 kyr BP (ref. 21). During continental deglaciation, sea levels rose slowly from about 19 kyr BP, then more rapidly from about 16 to 12.5 kyr BP (ref. 14). Widespread thaw of permafrost in NW Europe was instigated by slight warming at about 17–15 kyr BP then rapid warming at the start of the Late Glacial Interstadial about 14.7–12.9 kyr BP (ref. 21). There was a brief return to colder conditions (Younger Dryas/Greenland Stadial 1, about 12.9–11.7 kyr BP) before the present interglacial, the Holocene. After the Younger Dryas, sea-level rise was rapid, approaching present-day levels around 7 kyr BP (ref. 14).

Variations in herbivore collagen  $\delta^{34}\text{S}$  are typically interpreted as reflecting differences in animal spatial ecology, driven by differences in the  $\delta^{34}\text{S}$  of consumed plants with varying underlying geology and/or distance from coast. However, our data analysis shows that animal

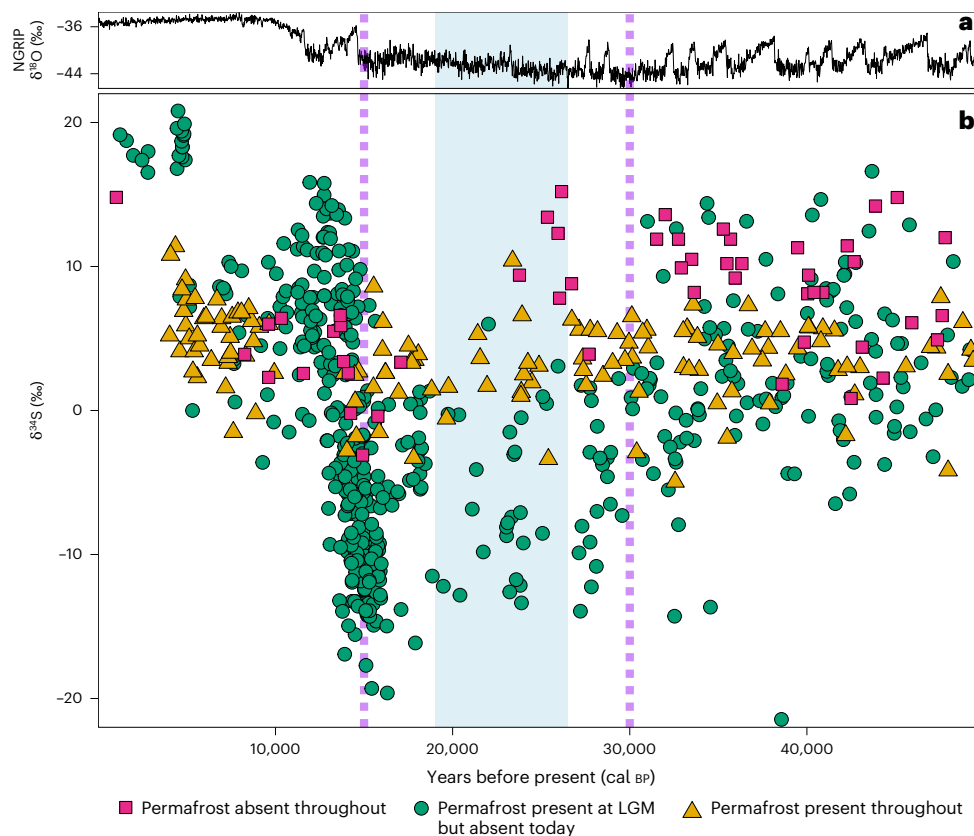


**Fig. 2 | Faunal collagen  $\delta^{34}\text{S}$  values from Eurasia through the Late Pleistocene and Holocene.** Each data point represents a single animal specimen, which has been directly radiocarbon dated. **a**, The North Greenland Ice Core Project (NGRIP) oxygen isotope record<sup>42</sup>, a proxy for global temperature. **b**, Faunal collagen  $\delta^{34}\text{S}$  values. Shaded blue area indicates approximate duration of the LGM. The dashed purple lines indicate approximate timing of continuous permafrost development

(about 30 kyr BP) and thaw (about 15 kyr BP) in western Eurasia. Pink squares: samples collected from regions where no permafrost was present during the last 50,000 years. Green circles: samples collected from areas that either had permafrost present at the LGM or were under ice sheets/glaciers at the LGM but where permafrost/ice is absent today. Yellow triangles: samples collected from regions in which permafrost has been present throughout the past 50,000 years.

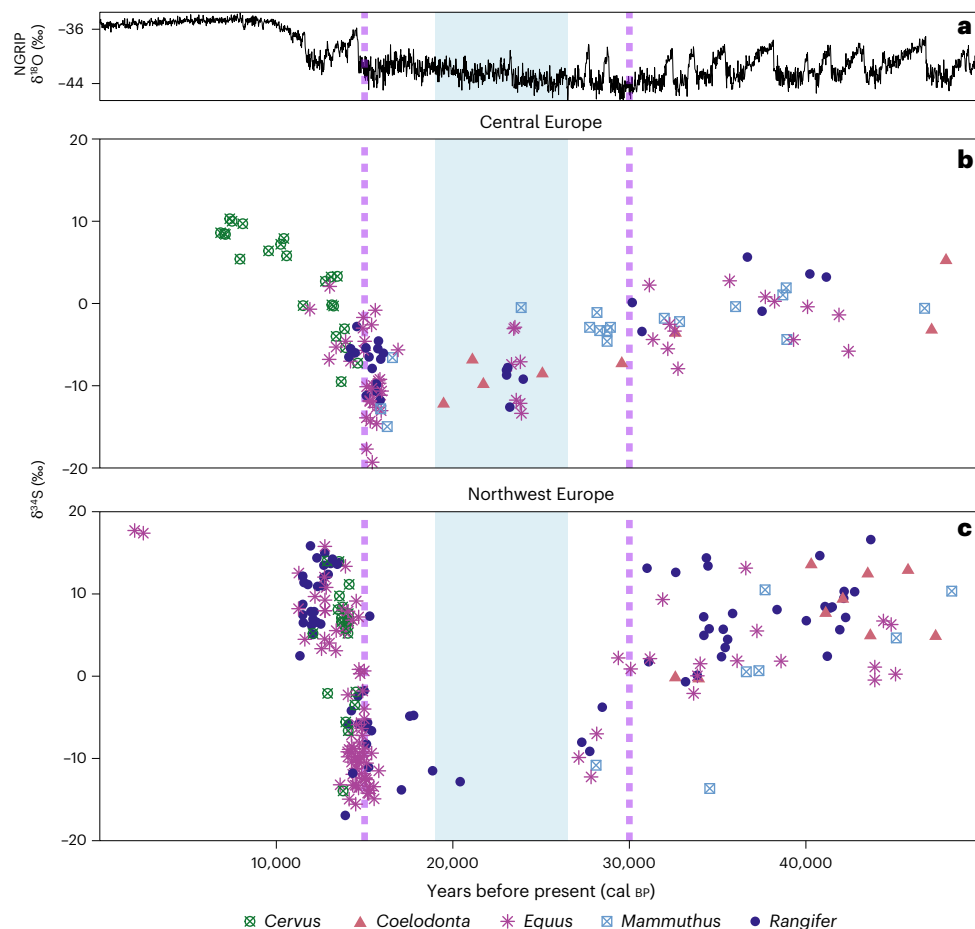


**Fig. 3 |  $\delta^{34}\text{S}$  values of radiocarbon-dated herbivores from central and northwest Europe for the five most abundant taxa in both regions, *Cervus elaphus*, *Coelodonta antiquitatis*, *Equus* sp., *Mammuthus primigenius* and *Rangifer tarandus*. a**, The Greenland ice-core oxygen isotope record, a proxy for global temperature<sup>42</sup>. **b, c**,  $\delta^{34}\text{S}$  values of radiocarbon-dated herbivores from

central and northwest Europe (46.5° N to 54° N, 6° E to 21° E) (**b**) and northwest Europe (50° N to 60° N, 10° E to 6° W) (**c**). Shaded blue area indicates approximate duration of the LGM. The dashed purple lines indicate approximate timing of continuous permafrost development (about 30 kyr BP) and widespread thaw (about 15 kyr BP) in western Eurasia.

spatial ecology is not the primary driver of the LPSE. There are many potential influences such as changes in atmospheric sulfur source (particularly loess and sea-spray) linked to sea-level variations, sulfur emissions from volcanic activity, changes in bedrock weathering rates linked to glaciation, temperature and precipitation changes (Supplementary Discussion 1.2 provides detailed discussion). However, our multivariate analysis concludes that changing near-surface permafrost conditions are the most plausible driver of the observed excursion (Supplementary Discussion 1.4).

Permafrost currently underlies substantial areas of Alaska, Canada, Siberia and Greenland and was present throughout the Late Pleistocene. During the LGM, permafrost expanded across northern Eurasia<sup>20</sup>. Its maximum extent has been established via mapping of permafrost-related geomorphological features<sup>22</sup>. Notably, our faunal  $\delta^{34}\text{S}$  values differ substantially between regions with different permafrost histories (Supplementary Discussion 1.4, Supplementary Tables 6 and 7 and Supplementary Fig. 11). The LPSE is observed exclusively in regions where permafrost (or ice sheets/alpine glaciers) was present during the LGM but are now permafrost free (Fig. 2) and coincides with the timing of regional permafrost development and thaw inferred from local geomorphological evidence<sup>22,23</sup> and Greenland ice cores<sup>24</sup> (Supplementary Fig. 1). The LPSE is not observed in regions where permafrost is present today and persisted throughout the Late Pleistocene (Figs. 1 and 2), nor in regions where permafrost was not present over the last 50 kyr (Supplementary Fig. 1).

We highlight two processes associated with permafrost thaw that may have driven the shift to lighter  $\delta^{34}\text{S}$  during the LPSE, both of which would have impacted plant (and therefore animal)  $\delta^{34}\text{S}$ : inputs from newly thawed substrate generated by active-layer deepening and the development of anoxic wetlands due to impeded drainage.

Permafrost growth impedes weathering of underlying bedrock and sediments. Active-layer deepening and thawing therefore increase the input of sedimentary sulfides and enhance sulfide oxidation<sup>25</sup>, transferring the negative sulfide  $\delta^{34}\text{S}$  signature to soils. Permafrost development also substantially influences hydrology, impeding drainage and confining soil water to the active layer, which can induce periodic waterlogged, anoxic soil conditions. Such conditions alter soil redox status, enhancing sulfide production via dissimilatory sulfate reduction (DSR) in bacteria and archaea<sup>26</sup>, a process that can produce large (–46 to –40‰) isotopic fractionation<sup>27</sup>. These low-sulfide  $\delta^{34}\text{S}$  values are inherited by plants after re-oxidation to sulfate<sup>28,29</sup>. Microbial DSR readily occurs in cold regions<sup>30–33</sup>, including areas of modern permafrost thaw<sup>34,35</sup>. Sufficiently cold temperatures, however, suppress the extent of DSR<sup>36</sup> and inhibit weathering, potentially explaining the lack of LPSE in regions with stable permafrost across the last 50,000 years (Supplementary Fig. 1 and Supplementary Data 1). It follows, therefore, that the LPSE is only observed in those lower-latitude regions subject to extensive climatic, environmental and permafrost perturbations. Intermediate temperatures (Supplementary Fig. 1 and Supplementary Data 1) and young, epigenetic permafrost<sup>37</sup> would have

enhanced weathering rates, sulfur availability and DSR throughout the Late Pleistocene, followed by extensive thaw after the LGM, producing the lowest  $\delta^{34}\text{S}$  values.

Further investigation into the spatio-temporal extent and continuity of these processes, including whether the LPSE is observed in other regions such as North America, is needed to assess the degree to which permafrost change drives the LPSE.

Modern permafrost is a major reservoir of organic carbon, which is being released to the atmosphere as  $\text{CO}_2$  and methane as the Arctic warms at twice the global average rate<sup>38</sup>, accelerating warming<sup>39</sup>. We can investigate permafrost sensitivity to climate shifts by studying the relationship between past permafrost conditions and palaeoclimate change. However, this is hindered by limited data on the timing of permafrost growth and thaw. The geomorphological features used to assess past permafrost extent are often difficult to date<sup>18</sup>. Our results show that sulfur isotope analysis of faunal samples could provide high-resolution records of past permafrost change because the preserved isotopic signature of bone collagen represents only a few years to decades of the animal's life, restricted to its home range, and bone collagen from the last about 50,000 years is directly dateable through radiocarbon methods with good preservation potential. The spatio-temporal patterns of these data allow insights into permafrost development and degradation at local to continental scales. More broadly, our findings indicate animal  $\delta^{34}\text{S}$  values can reflect changes in local hydrology and loess deposition, complicating the use of  $\delta^{34}\text{S}$  as a provenancing tool for food origin, animal migration and archaeological research. This issue will not arise in faunal datasets of similar age, with stable permafrost, hydrology and loess deposition. Furthermore, these findings support the utility of sulfur isotopes to examine wetland habitat use by people and animals in modern and archaeological contexts.

## Online content

Any methods, additional references, Nature Portfolio reporting summaries, source data, extended data, supplementary information, acknowledgements, peer review information; details of author contributions and competing interests; and statements of data and code availability are available at <https://doi.org/10.1038/s41561-025-01760-x>.

## References

- Krouse, R., Mayer, B. & Schoenau, J. J. in *Mass Spectrometry of Soils* (eds Boutton, T. & Yamasaki, S.) 247–284 (Marcel Dekker, 1996).
- Nielsen, H. Isotopic composition of the major contributors to atmospheric sulfur. *Tellus* **26**, 213–221 (1974).
- Stevens, R. E. et al. Iso-wetlands: unlocking wetland ecologies and agriculture in prehistory through sulfur isotopes. *Archaeol. Int.* **25**, 168–176 (2022).
- Lamb, A. L., Chenery, C. A., Madgwick, R. & Evans, J. A. Wet feet: developing sulfur isotope provenance methods to identify wetland inhabitants. *R. Soc. Open Sci.* **10**, 230391 (2023).
- Peterson, B. J., Howarth, R. W. & Garritt, R. H. Multiple stable isotopes used to trace the flow of organic matter in estuarine food webs. *Science* **227**, 1361–1363 (1985).
- Richards, M. P., Fuller, B. T., Sponheimer, M., Robinson, T. & Ayliffe, L. Sulphur isotopes in palaeodietary studies: a review and results from a controlled feeding experiment. *Int. J. Osteoarchaeol.* **13**, 37–45 (2003).
- Trust, B. A. & Fry, B. Stable sulphur isotopes in plants: a review. *Plant Cell Environ.* **15**, 1105–1110 (1992).
- White, J. R. & Reddy, K. R. in *The Wetlands Handbook* (eds Maltby, E. & Barker, T.) 213–227 (Wiley-Blackwell, 2009).
- Reade, H. et al. Deglacial landscapes and the Late Upper Palaeolithic of Switzerland. *Quat. Sci. Rev.* **239**, 106372 (2020).
- Reade, H. et al. Magdalenian and Epimagdalenian chronology and palaeoenvironments at Kůlna Cave, Moravia, Czech Republic. *Archaeol. Anthropol. Sci.* **13**, 4 (2021).
- Stevens, R. E., Reade, H., Tripp, J., Sayle, K. A. & Walker, E. A. in *The Beef Behind All Possible Pasts. The Tandem-Festschrift in Honour of Elaine Turner and Martin Street* (ed. Saudzinski-Windheuser S, J. O.) 589–607 (Römisch-Germanischen Zentralmuseums, 2021).
- Wißing, C. et al. Stable isotopes reveal patterns of diet and mobility in the last Neandertals and first modern humans in Europe. *Sci. Rep.* **9**, 4433 (2019).
- Dansgaard, W. et al. Evidence for general instability of past climate from a 250-kyr ice-core record. *Nature* **364**, 218–220 (1993).
- Lambeck, K., Yokoyama, Y. & Purcell, T. Into and out of the Last Glacial Maximum: sea-level change during oxygen isotope stages 3 and 2. *Quat. Sci. Rev.* **21**, 343–360 (2002).
- Vandenberghe, J., Lowe, J., Coope, G. R., Litt, T. & Zöller, L. In *Past Climate Variability through Europe and Africa PEPIII Conference Proceedings* (eds Battarbee, R. et al.) 393–416 (Kluwer, 2004).
- Vandenberghe, J. & van der Plicht, J. The age of the Hengelo interstadial revisited. *Quat. Geochronol.* **32**, 21–28 (2016).
- Helmens, K. F. The last interglacial–glacial cycle (MIS 5–2) re-examined based on long proxy records from central and northern Europe. *Quat. Sci. Rev.* **86**, 115–143 (2014).
- Hughes, A. L. C., Gyllencreutz, R., Lohne, Ø. S., Mangerud, J. & Svendsen, J. I. The last Eurasian ice sheets—a chronological database and time-slice reconstruction, DATED-1. *Boreas* **45**, 1–45 (2016).
- Lambeck, K., Rouby, H., Purcell, A., Sun, Y. & Sambridge, M. Sea level and global ice volumes from the Last Glacial Maximum to the Holocene. *Proc. Natl Acad. Sci. USA* **111**, 15296–15303 (2014).
- Lindgren, A., Hugelius, G., Kuhry, P., Christensen, T. R. & Vandenberghe, J. GIS-based maps and area estimates of northern hemisphere permafrost extent during the last glacial maximum. *Permafrost Periglacial Processes* **27**, 6–16 (2015).
- Kasse, C., Vandenberghe, D., De Corte, F. & Van Den Haute, P. Late Weichselian fluvio-aeolian sands and coversands of the type locality Grubbenvorst (southern Netherlands): sedimentary environments, climate record and age. *J. Quat. Sci.* **22**, 695–708 (2007).
- Vandenberghe, J. et al. The Last Permafrost Maximum (LPM) map of the Northern Hemisphere: permafrost extent and mean annual air temperatures, 25–17 ka BP. *Boreas* **43**, 652–666 (2014).
- Bertran, P. Distribution and characteristics of Pleistocene ground thermal contraction polygons in Europe from satellite images. *Permafrost Periglacial Processes* **33**, 99–113 (2022).
- Wolff, E. W., Chappellaz, J., Blunier, T., Rasmussen, S. O. & Svensson, A. Millennial-scale variability during the last glacial: the ice core record. *Quat. Sci. Rev.* **29**, 2828–2838 (2010).
- Zolkos, S., Tank, S. E. & Kokelj, S. V. Mineral weathering and the permafrost carbon-climate feedback. *Geophys. Res. Lett.* **45**, 9623–9632 (2018).
- Postgate, J. Sulphate reduction by bacteria. *Annu. Rev. Microbiol.* **13**, 505–520 (1959).
- Kemp, A. L. W. & Thode, H. G. The mechanism of the bacterial reduction of sulphate and of sulphite from isotope fractionation studies. *Geochim. Cosmochim. Acta* **32**, 71–91 (1968).
- Chambers, L. A. & Trudinger, P. A. Microbiological fractionation of stable sulfur isotopes: a review and critique. *Geomicrobiol. J.* **1**, 249–293 (1979).
- Toran, L. & Harris, R. F. Interpretation of sulfur and oxygen isotopes in biological and abiological sulfide oxidation. *Geochim. Cosmochim. Acta* **53**, 2341–2348 (1989).
- Van Stempvoort, D. & Biggar, K. Potential for bioremediation of petroleum hydrocarbons in groundwater under cold climate conditions: a review. *Cold Reg. Sci. Technol.* **53**, 16–41 (2008).
- Van Stempvoort, D. R. et al. Sulfate in streams and groundwater in a cold region (Yukon Territory, Canada): evidence of weathering processes in a changing climate. *Chem. Geol.* **631**, 121510 (2023).



32. Ansari, A. H. Stable isotopic evidence for anaerobic maintained sulphate discharge in a polythermal glacier. *Polar Sci.* **10**, 24–35 (2016).
33. Hindshaw, R. S., Heaton, T. H. E., Boyd, E. S., Lindsay, M. R. & Tipper, E. T. Influence of glaciation on mechanisms of mineral weathering in two high Arctic catchments. *Chem. Geol.* **420**, 37–50 (2016).
34. Jones, E. L. et al. Biogeochemical processes in the active layer and permafrost of a high Arctic fjord valley. *Front. Earth Sci.* **8**, 342 (2020).
35. Kemeny, P. C. et al. Arctic permafrost thawing enhances sulfide oxidation. *Glob. Biogeochem. Cycles* **37**, (2023).
36. Mitchell, K., Heyer, A., Canfield, D. E., Hoek, J. & Habicht, K. S. Temperature effect on the sulfur isotope fractionation during sulfate reduction by two strains of the hyperthermophilic *Archaeoglobus fulgidus*. *Environ. Microbiol.* **11**, 2998–3006 (2009).
37. French, H. & Shur, Y. The principles of cryostratigraphy. *Earth Sci. Rev.* **101**, 190–206 (2010).
38. Schuur, E. A. G., McGuire, A. D., Schädel, C. & Grosse, G. Climate change and the permafrost carbon feedback. *Nature* **520.7546**, 171–179 (2015).
39. Zimov, S. A., Schuur, E. A. G. & Chapin, F. S. Permafrost and the global carbon budget. *Science* **312**, 1612–1613 (2006).
40. Becker, D., Verheul, J., Zickel, M. & Willmes, C. LGM paleoenvironment of Europe–map. *University of Cologne* <https://doi.org/10.5880/SFB806.15> (2015).
41. Brown, J., Ferrians, O., Heginbottom, J. A. & Melnikov, E. Circum-arctic map of permafrost and ground ice conditions, ver. 2. *National Snow and Ice Data Center* <https://doi.org/10.7265/skbg-kf16> (2002).
42. North Greenland Ice Core Project members. High-resolution record of Northern Hemisphere climate extending into the last interglacial period. *Nature* **431**, 147–151 (2004).

**Publisher's note** Springer Nature remains neutral with regard to jurisdictional claims in published maps and institutional affiliations.

**Open Access** This article is licensed under a Creative Commons Attribution 4.0 International License, which permits use, sharing, adaptation, distribution and reproduction in any medium or format, as long as you give appropriate credit to the original author(s) and the source, provide a link to the Creative Commons licence, and indicate if changes were made. The images or other third party material in this article are included in the article's Creative Commons licence, unless indicated otherwise in a credit line to the material. If material is not included in the article's Creative Commons licence and your intended use is not permitted by statutory regulation or exceeds the permitted use, you will need to obtain permission directly from the copyright holder. To view a copy of this licence, visit <http://creativecommons.org/licenses/by/4.0/>.

© The Author(s) 2025

## Methods

Our dataset comprises 796  $\delta^{34}\text{S}$  isotope analyses (510 new and 286 previously published  $\delta^{34}\text{S}$  values (Supplementary Data 1). New  $\delta^{34}\text{S}$  analyses were undertaken on collagen extracted from 395 bones and 115 teeth sourced from 68 archaeological/palaeontological sites ( $n = 1$  to 56 samples per site). Of our 510 new  $\delta^{34}\text{S}$  analyses, 221 were carried out on collagen previously extracted at Oxford Radiocarbon Accelerator Unit (ORAU) for radiocarbon dating; 221 were carried out on collagen previously extracted for our previous studies<sup>43–50</sup> and 68 on collagen extracted for this study. The method of collagen extraction for each sample is given in Supplementary Data 1 and fully described in our recent study<sup>44</sup>. Only data with C/S and N/S ratios indicative of well-preserved collagen were compiled from the literature<sup>51,52</sup>. Genus/species represented in our dataset include *Bos/Bison* sp., *Capreolus capreolus*, *Cervus elaphus*, *Alces alces*, *Coelodonta antiquitatis*, *Equus* sp., *Mammuthus primigenius*, *Megaloceros giganteus*, *Ovibos moschatus*, *Ovis aries*, *Rangifer tarandus*, *Rupicapra*, *Saiga tatarica* and *Sus* (Supplementary Data 1). New AMS determinations were undertaken at ORAU for 25 samples, and 666 of the samples had previously been radiocarbon dated by AMS. Sample details and preparation methods are given in Supplementary Data 1 and Supplementary Discussion 1. Sulfur isotope ratios were determined on the extracted collagen using a Delta V Advantage continuous-flow isotope ratio mass spectrometer coupled via a ConFloIV to an IsoLink elemental analyser (Thermo Scientific) at the Scottish Universities Environmental Research Centre. Samples were weighed into tin capsules (~1.2–1.5 mg) and combusted in the presence of oxygen in a single reactor containing tungstic oxide and copper wires at 1,020 °C to produce  $\text{SO}_2$ . A magnesium perchlorate trap was used to eliminate water produced during the combustion process, and the gas was separated in a gas chromatography column heated between 70 °C and 240 °C. Helium was used as a carrier gas throughout the procedure.  $\text{SO}_2$  entered the mass spectrometer via an open split arrangement within the ConFloIV and was analysed against a reference gas. Samples were analysed in duplicate, with the exception of 16 samples for which there was only sufficient collagen for a single analysis. For every ten unknown archaeological samples, either three gelatine-based in-house standards (SAG:  $\delta^{34}\text{S}_{\text{VCDT}} = -10.1 \pm 0.1\text{‰}$ , MAG:  $\delta^{34}\text{S}_{\text{VCDT}} = 1.4 \pm 0.1\text{‰}$  and MSAG:  $\delta^{34}\text{S}_{\text{VCDT}} = 11.1 \pm 0.1\text{‰}$ ) or two gelatine-based in-house standards (SAG2B:  $\delta^{34}\text{S}_{\text{VCDT}} = -9.5 \pm 0.1\text{‰}$  and MSAG2:  $\delta^{34}\text{S}_{\text{VCDT}} = 11.5 \pm 0.1\text{‰}$ ), which were calibrated to the International Atomic Energy Agency (IAEA) reference materials IAEA-S-1 (silver sulfide,  $\delta^{34}\text{S}_{\text{VCDT}} = -0.3 \pm 0.2\text{‰}$ ), IAEA-S-2 (silver sulfide,  $\delta^{34}\text{S}_{\text{VCDT}} = 22.7 \pm 0.2\text{‰}$ ), IAEA-SO-5 (barium sulfate,  $\delta^{34}\text{S}_{\text{VCDT}} = 0.5 \pm 0.2\text{‰}$ ) and IAEA-SO-6 (barium sulfate,  $\delta^{34}\text{S}_{\text{VCDT}} = -34.1 \pm 0.2\text{‰}$ ) were used to normalize the  $\delta^{34}\text{S}_{\text{VCDT}}$  values. Results are reported as per mille (‰) relative to the internationally accepted standard Vienna Canyon Diablo Troilite (VCDT). Normalization was checked using United States Geological Survey (USGS) reference material USGS43 (Indian human hair:  $\delta^{34}\text{S}_{\text{VCDT}} = 10.5 \pm 0.2\text{‰}$ ) or the well-characterized Elemental Microanalysis Isotope Ratio Mass Spectrometry fish gelatin standard B2215 ( $\delta^{34}\text{S}_{\text{VCDT}} = 1.2 \pm 0.2\text{‰}$ ), and long-term precision was determined to  $\pm 0.4\text{‰}$  for  $\delta^{34}\text{S}$  based on repeated measurements of an Iron Age in-house horse bone collagen standard (DHB2019:  $\delta^{34}\text{S}_{\text{VCDT}} = 9.5 \pm 0.2\text{‰}$ ,  $n = 1,246$ ). All our samples had C/S and N/S ratios (306–898 and 100–284) within the quality range indicative of well-preserved collagen for sulfur isotope analysis<sup>51</sup>. Statistical analyses were undertaken in R version 4.3.0 to explore potential drivers of the LPSE. Parameters considered include underlying geology, proximity to loessic deposits, proximity to palaeocoastlines, proximity to palaeo-ice sheets, modelled mean annual temperature and precipitation, proximity to present-day and LGM permafrost. Data were investigated using Kruskal–Wallis tests and factor analysis of mixed data, which considers continuous and categorical variables within the same model (full details of statistical analyses are given in Supplementary Data 1). A hierarchical cluster analysis of the three most important components from the factor analysis of mixed data analysis was conducted (Supplementary Fig. 13), identifying subgroups in the data that share similar characteristics,

exploring variables contributing to the  $\delta^{34}\text{S}$  trends. The identified clusters were then considered in relation to the temporal trend observed in the  $\delta^{34}\text{S}$  data.

## Data availability

All data are available at <https://doi.org/10.5522/04/28677713> (ref. 52) and in the Supplementary Information accompanying this article.

## References

- Stevens, R. E. *Establishing Links Between Climate/environment and Both Modern and Archaeological Hair and Bone Isotope Values: Determining the Potential of Archaeological Bone Collagen  $\delta^{13}\text{C}$  and  $\delta^{15}\text{N}$  as Palaeoclimatic and Palaeoenvironmental Proxies*. Ph.D thesis, Univ. of Oxford (2005).
- Reade, H. et al. Nitrogen palaeo-isoscapes: changing spatial gradients of faunal  $\delta^{15}\text{N}$  in late Pleistocene and early Holocene Europe. *PLoS ONE* **18**, e0268607 (2023).
- Stevens, R. E., O'Connell, T. C., Hedges, R. E. M. & Street, M. Radiocarbon and stable isotope investigations at the central Rhineland sites of Gönnersdorf and Andernach-Martinsberg, Germany. *J. Hum. Evol.* **57**, 131–148 (2009).
- Germonpré, M. et al. Fossil dogs and wolves from Palaeolithic sites in Belgium, the Ukraine and Russia: osteometry, ancient DNA and stable isotopes. *J. Archaeol. Sci.* **36**, 473–490 (2009).
- Stevens, R. E., Germonpré, M., Petrie, C. A. & O'Connell, T. C. Palaeoenvironmental and chronological investigations of the Magdalenian sites of Goyet Cave and Trou de Chaleux (Belgium), via stable isotope and radiocarbon analyses of horse skeletal remains. *J. Archaeol. Sci.* **36**, 653–662 (2009).
- Stevens, R. E. & Hedges, R. E. M. Carbon and nitrogen stable isotope analysis of northwest European horse bone and tooth collagen, 40,000 BP–present: palaeoclimatic interpretations. *Quat. Sci. Rev.* **23**, 977–991 (2004).
- Stevens, R. E. et al. Nitrogen isotope analyses of reindeer (*Rangifer tarandus*), 45,000 BP to 9,000 BP: palaeoenvironmental reconstructions. *Palaeogeogr. Palaeoclimatol. Palaeoecol.* **262**, 32–45 (2008).
- Stevens, R. E., Jacobi, R. M. & Higham, T. F. G. Reassessing the diet of Upper Palaeolithic humans from Gough's Cave and Sun Hole, Cheddar Gorge, Somerset, UK. *J. Archaeol. Sci.* **37**, 52–61 (2010).
- Nehlich, O. & Richards, M. P. Establishing collagen quality criteria for sulphur isotope analysis of archaeological bone collagen. *Archaeol. Anthropol. Sci.* **1**, 59–75 (2009).
- Stevens, R. E. et al. Research data for 'sulfur isotope excursions in Eurasia during the last glacial linked to permafrost change'. *UCL Research Data Repository* <https://doi.org/10.5522/04/28677713> (2025).

## Acknowledgements

This research was funded by an ERC Consolidator Grant awarded to R.E.S. (grant number 617777) and a Leverhulme Trust Research Project Grant to R.E.S., S.H.B. and J.B.M. (RPG-2021-254). This work was made possible by the support of a great many colleagues and institutes, who facilitated access to and permitted sampling of numerous archaeological and palaeontological collections. We would like to thank R. Jacobi; C. Stringer and the Ancient Human Occupation of Britain project; S. Grimm; S. Charlton; M. Marr; T. Lord; T. O'Connor; L. Wilson; G. Mullan and the University of Bristol Spelaeological Society Museum; B. Chandler and Torquay Museum; J. Freedman and Plymouth City Museum and Art Gallery; B. Lewarne and the Devon Karst Society; the Museum of Archaeology and Anthropology, Cambridge; the Potteries Museum and Art Gallery, Stoke-on-Trent; Buxton Museum and Art Gallery; E. Walker and the National Museum Cardiff; R. Miller; the University of Liege; A. Folie and the Royal Belgian Institute of Natural Sciences; P. Neruda; Z. Nerudova; M. Roblíčková

and the Moravian Museum; A. Pryor; J. Svoboda; N. Conard; S. Münzel; Wells and Mendips Museum, Somerset; S. Pappa; P. Brewer and the Natural History Museum London; L. Astill and Creswell Crags Museum and Prehistoric Gorge; Sheffield Museums; T. Terberger; P. Wotjal; M. Poltowicz-Bobak; D. Bobak; and the Institute of Systematic and Evolution of Animals, Polish Academy of Sciences and P. Ditchfield, ORAU. R. Madgwick, A. Lamb and S. Wexler are thanked for their helpful discussions concerning sulfur isotopes.

### Author contributions

R.E.S. conceived of the project. R.E.S. and H.R. contributed to the project design. R.E.S., H.R., A.L., M.G., M.S. and T.F.G.H. contributed or provided access to samples for analysis. R.E.S., H.R., K.L.S., J.A.T., D.F. and T.F.G.H. generated data. R.E.S. and H.R. analysed data. R.E.S., H.R., J.A.T., D.F., J.B.M. and S.H.B. contributed to the interpretation of results. R.E.S. wrote the original paper draft. R.E.S., H.R., K.L.S., J.A.T., D.F., A.L., I.B., M.G., M.S., J.B.M., S.H.B., T.F.G.H. and D.H.J. reviewed and edited the paper. R.E.S., I.B., J.B.M., S.H.B. and T.F.G.H. acquired funding for the project.

### Competing interests

The authors declare no competing interests.

### Additional information

**Supplementary information** The online version contains supplementary material available at <https://doi.org/10.1038/s41561-025-01760-x>.

**Correspondence and requests for materials** should be addressed to Rhiannon E. Stevens.

**Peer review information** *Nature Geoscience* thanks Clement Bataille and Peter Wynn for their contribution to the peer review of this work. Primary Handling Editor: James Super, in collaboration with the *Nature Geoscience* team.

**Reprints and permissions information** is available at [www.nature.com/reprints](http://www.nature.com/reprints).